Quaternary Science Reviews 71 (2013) 70–80

Contents lists available at SciVerse ScienceDirect

Quaternary Science Reviews

journal homepage: www.elsevier.com/locate/quascirev

Luminescence dating of the PASADO core 5022-1D from Laguna Potrok Aike (Argentina) using IRSL signals from feldspar

J.-P. Buylaert [a,b,*], A.S. Murray [a], A.C. Gebhardt [c], R. Sohbati [a], C. Ohlendorf [d], C. Thiel [a,b], S. Wastegård [e], B. Zolitschka [d], The PASADO Science Team [1]

[a] Nordic Laboratory for Luminescence Dating, Department of Geoscience, Aarhus University, DTU Risø Campus, DK-4000 Roskilde, Denmark
[b] Technical University of Denmark, Center for Nuclear Technologies, DTU Risø Campus, Building 201, Frederiksborgvej 399, DK-4000 Roskilde, Denmark
[c] Alfred Wegener Institute Helmholtz Centre for Polar and Marine Research, 27568 Bremerhaven, Germany
[d] Institute of Geography, University of Bremen, 28359 Bremen, Germany
[e] Department of Physical Geography and Quaternary Geology, Stockholm University, SE-10691 Stockholm, Sweden

ARTICLE INFO

Article history:
Received 14 August 2012
Received in revised form
6 March 2013
Accepted 22 March 2013
Available online 3 May 2013

Keywords:
Luminescence
K-feldspar
Post-IR IRSL
Bleaching
ICDP-project PASADO

ABSTRACT

We have measured and tested a luminescence chronology for the PASADO core 5022-1D from the maar lake of Laguna Potrok Aike. Because of unsuitable quartz OSL characteristics, sand-sized K-feldspar extracts were chosen as a dosimeter and the dose was measured using a post-IR IRSL ($pIRIR_{290}$) measurement protocol. Using this approach we were able to access a stable signal and thus avoid the ubiquitous problem of feldspar signal instability. Extensive laboratory tests show that the chosen $pIRIR_{290}$ protocol is applicable to these samples. We also developed a new criterion based on known relative bleaching rates of the conventional IRSL signal (IR_{50}) and the $pIRIR_{290}$ signal and the relationship between resulting equivalent doses; this is used to identify and reject poorly bleached samples. Eighteen samples out of 47 were rejected based on this criterion, without reference to absolute doses or stratigraphy; the resulting age–depth profile is self-consistent, increases smoothly with depth and is in agreement with independent age control based on volcanic ash layers (Reclús, Mt Burney and Hudson tephras) at the top and middle of the core. Our new luminescence chronology suggests that the 5022-1D core reaches back to ~65 ka at ~96 m below lake floor.

1. Introduction

Laguna Potrok Aike in Southern Argentina contains a southern hemisphere archive of climate change. The lake is located in the rain shadow of the Andes with a highly variable modern annual precipitation ranging from <150 to 300 mm (Mayr et al., 2007; Ohlendorf et al., 2013); it is strongly influenced by southern hemisphere westerly winds and is very sensitive to moisture changes (e.g. Anselmetti et al., 2009). Laguna Potrok Aike is a maar lake with a relatively small contribution from the catchment; as a result the sediment column is likely to have recorded a regional climate signal (Zolitschka et al., 2006). However, this record cannot be related to other global climate records without a reliable chronology. Both radiocarbon and luminescence dating have been applied to Laguna Potrok Aike sediments (Haberzettl et al., 2009; Kliem et al., 2013b). Haberzettl et al. (2009) point out the potential of luminescence dating to provide an absolute chronology beyond the radiocarbon dating limit (~40 ka) but 5 out of 6 luminescence ages they present underestimate significantly when compared to independent age control (see Figs. 3 and 5 in Haberzettl et al., 2009).

Recent advances in the understanding of feldspar as a luminescence dosimeter (Thomsen et al., 2008, 2011; Murray et al., 2009; Jain and Ankjærgaard, 2011) have led to new single-aliquot regenerative dose (SAR) dating protocols for feldspar (so called post-IR IRSL protocols; e.g. Buylaert et al., 2009; Thiel et al., 2011); these minimise or even completely remove the effect of anomalous fading and have been shown to give accurate ages (Li and Li, 2011; Reimann et al., 2011; Buylaert et al., 2012). In this paper we employ the post-IR IRSL protocol proposed by Thiel et al. (2011) and Buylaert et al. (2012) to derive a luminescence-based chronology for the PASADO 5022-1D core. The luminescence characteristics of this signal are discussed in detail and we show, for the first time,

* Corresponding author. Nordic Laboratory for Luminescence Dating, Department of Geoscience, Aarhus University, DTU Risø Campus, DK-4000 Roskilde, Denmark. Tel.: +45 4677 4926.
E-mail address: jabu@dtu.dk (J.-P. Buylaert).

[1] PASADO Science Team as cited at: http://www.icdp-online.org/front_content.php?idcat=1494.

0277-3791/$ – see front matter © 2013 Elsevier Ltd. All rights reserved.
http://dx.doi.org/10.1016/j.quascirev.2013.03.018

how to employ the different bleaching rates of the IRSL and post-IR IRSL signals to identify those samples that are most likely fully bleached in nature and hence likely to yield the most reliable ages. Finally, the preferred age–depth dataset is compared with available independent age control.

2. Background

Luminescence dating is a widely applicable trapped charge dating method which can be used to determine the time that has elapsed since sediment grains (quartz, feldspars) were last exposed to daylight (Aitken, 1998). During burial, quartz and feldspar grains absorb energy from ionising radiation due to the natural radiation flux (alpha, beta, gamma) from radionuclides (U-, Th-series, ^{40}K) present in the sediment. Some of this energy is stored as trapped charge within the crystal structure. When these grains are exposed to daylight, e.g. during erosion and/or transport, some of the trapped energy is released (solar resetting of the luminescence signal); during subsequent burial the trapped charge (a function of the cumulative radiation dose) builds up again. In the laboratory a part of this trapped charge is released by thermal or optical stimulation and gives rise to a luminescence signal (called thermoluminescence (TL) in the case of thermal stimulation and optically stimulated luminescence (OSL) in the case of optical stimulation). By means of a dose response curve, the natural luminescence signal can be compared to luminescence signals induced artificially using a radiation source; interpolation of the natural luminescence onto the dose response curve gives the burial dose, or equivalent dose (D_e in Gy, 1 Gy = 1 J/kg). By dividing the burial dose by the dose rate (in Gy/ka, derived from radionuclide concentrations in the sediment) the time since last daylight exposure is obtained. Two important factors (*inter alia*) influence the accuracy of a luminescence age: (i) complete removal (or bleaching) during transport prior to burial of any trapped charge that the grains may carry – incomplete removal will cause age overestimation, (ii) the cumulative charge is trapped at stable sites during burial – instability will cause age underestimation.

3. Site description and age control

Laguna Potrok Aike is located at 52°S, 70°W in the Patagonian steppe region at an elevation of 113 m above sea level, some 100 km north of the Strait of Magellan. It is almost circular with a diameter of ~3.5 km and has a bowl-like shape with a shoulder at −33 m, steep slopes and a large central plain at 100 m water depth. The lake is currently fed by an ephemeral inlet at its western shore. Terraces that originate from former lake-level highstands of up to 21 m above present-day lake level are exposed and have been dated to Glacial (>17 ka) and Lateglacial (10–17 ka) (Kliem et al., 2013a). A lowstand during the early to mid Holocene was detected in sub-bottom echosounder profiles at −33 m below present-day lake level (Anselmetti et al., 2009). A complete desiccation, probably during Marine Isotope Stage 4 (MIS4), was postulated based on seismic reflection data (Gebhardt et al., 2012). Laguna Potrok Aike is situated within the range of tephra plumes from Andean volcanoes such as Hudson, Reclús and Mt. Burney. Thus, some prominent tephra layers are found in the lacustrine sediments and in outcrops around the lake (Kliem et al., 2013a).

During an ICDP (International Continental scientific Drilling Program) deep drilling campaign in austral summer 2008, seven cores were retrieved from two different drill sites (in quadruplicate and triplicate for Sites 1 and 2, respectively; Zolitschka et al., 2009, 2013) that were tentatively correlated (Recasens et al., 2012). Following the description of the composite profile of Site 2 (Kliem et al., 2013b), the lacustrine sediments of Laguna Potrok Aike are divided into two major units: the upper approximately 18 m are dominated by pelagic laminated silts, while in the lower part increasing amounts of turbidites and other type of mass movement deposits are intercalated with depth. The sediments of the upper unit are brownish to black, while they are greyish in the lower part (Ohlendorf et al., 2011). The upper unit contains varying amounts of total inorganic carbon (0–~4%; Haberzettl et al., 2007), while the lower part is almost free of inorganic carbon (Recasens et al., 2012; Hahn et al., 2013).

Our paper is based on samples taken from core 5022-1D (Fig. 1); the sediment/water interface was not recovered at this location and it is estimated that there is up to 1 m of material missing at the top. Three post-LGM tephra layers (Haberzettl et al., 2009) have been unambiguously identified in this core (Fig. 1): the Hudson tephra (7.16 m; 7.72 ± 0.14 ka cal. BP), Mt. Burney tephra (9.71 m; 9.44 ± 0.64 ka cal. BP) and Reclús tephra (14.15 m; 15.12 ± 0.45 ka cal. BP) (ages from Stern, 2008, summarised in Kliem et al., 2013b). A further Mt. Burney tephra layer (1T39: 49 ± 5 ka cal. BP; Kliem et al., 2013b) is present at 61.77 m hole depth in core 5022-1D. This tephra has also been identified at an

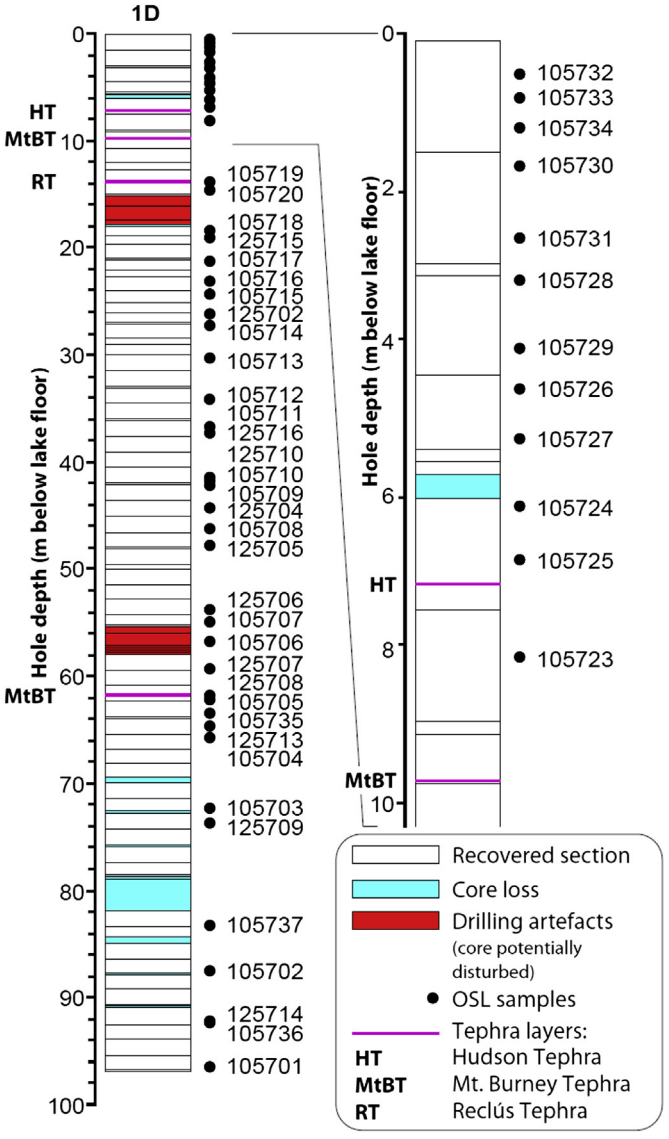

Fig. 1. Schematic 5022-1D core log (after Ohlendorf et al., 2011) showing luminescence sample positions and codes.

adjacent terrestrial site within the lake catchment and bracketing $pIRIR_{290}$ ages are consistent with these radiocarbon ages (Kliem et al., 2013a).

4. Methods

4.1. Methodological background

The majority of conventional luminescence ages are based on the fast-component-dominated quartz OSL signal measured using the single-aliquot regenerative-dose (SAR) procedure (Murray and Wintle, 2000; Wintle and Murray, 2006). The accuracy of this approach has been proven in several studies with independent age control (e.g. Murray and Olley, 2002; Duller, 2004; Vandenberghe et al., 2004; Madsen and Murray, 2009). One criterion for an accurate measurement of the dose using quartz OSL (Wintle and Murray, 2006) is the presence of a dominant fast component (Jain et al., 2003; Singarayer and Bailey, 2003). This signal is known to be rapidly bleachable by daylight to very low levels (e.g. Madsen and Murray, 2009) and is considered stable on the timescales of most dating applications (e.g. Murray and Wintle, 1999). Unfortunately, quartz with suitable characteristics is not always available (see review by Preusser et al., 2009) and the fast-component dose–response curve saturates at ~200 Gy, usually limiting its application to sediments not much older than ~100 ka (Wintle, 2008).

Feldspar luminescence grows to much higher doses than quartz OSL and thus has the potential to date older sediments, but unfortunately most feldspar signals are not stable. K-feldspars are sensitive to infrared (IR) light and generate infrared stimulated luminescence (IRSL). There is now abundant published evidence that conventional IRSL (from both K-rich feldspar extracts and polymineral fine-grains) measured with the sample held at or above ambient temperature (~50 °C) is affected by athermal fading (e.g. Huntley and Lamothe, 2001; Lamothe, 2004; Huntley and Lian, 2006; Buylaert et al., 2007, 2011a, 2012; Wallinga et al., 2007; Li et al., 2008; Davids et al., 2010; Madsen et al., 2011; Reimann et al., 2011). This unexpected instability is attributed to quantum-mechanical tunnelling and is usually called anomalous fading (Wintle, 1973; Aitken, 1985; Spooner, 1994). Without correction for this instability, feldspar ages typically underestimate the true burial age of the sediment (Huntley and Lamothe, 2001; Buylaert et al., 2011a). However, these corrections are usually large (typically 30–40%) and are based on untestable assumptions (Morthekai et al., 2008). Furthermore, Huntley and Lamothe (2001) argue that their correction model should not be used on samples exceeding 20–50 ka which limits its application to relatively young sediments. Feldspar dating is further complicated by the fact that IRSL signals are reset by daylight more slowly than quartz OSL (Godfrey-Smith et al., 1988; Thomsen et al., 2008; Buylaert et al., 2012; Murray et al., 2012); in non-favourable bleaching environments (e.g. fluvial or lacustrine systems) this could lead to incomplete resetting of IRSL signal. This can compensate for the effect of fading or even lead to age overestimations.

There are several applications of feldspar IRSL dating to lake cores (Lang and Zolitschka, 2001; Shulmeister et al., 2001; Thomas et al., 2003; Forman et al., 2007; Juschus et al., 2007; Moska et al., 2008; Haberzettl et al., 2009). In these studies the fine-silt (4–11 μm) polymineral fraction was used and IRSL was detected at or close to ambient temperature (from room temperature up to ~60 °C) in the blue (~400 nm) region of the wavelength spectrum (except for Thomas et al., 2003; Moska et al., 2008, which used UV detection). Some of these studies explain observed age underestimations by the presence of anomalous fading in their samples (Thomas et al., 2003; Moska et al., 2008; Haberzettl et al., 2009), other studies state that anomalous fading has only a small effect on the ages, if any (Shulmeister et al., 2001; Juschus et al., 2007). Lang and Zolitschka (2001) and Forman et al. (2007) claim that, in their samples, no significant anomalous fading could be detected. It should be noted that the effect of anomalous fading can be reduced – but not eliminated – by inserting a long delay between irradiation and measurement (e.g. Lang and Zolitschka, 2001; Forman et al., 2007) thus allowing the artificially induced luminescence signal to fade. Such an experimental procedure can reduce the apparent importance of anomalous fading, but it also makes an already small effect (on a laboratory time scale) much harder to detect and measure. Nevertheless, the effect on much longer geological timescales will still be significant. In addition, several of these studies have suggested that for some of the samples incomplete bleaching is likely to explain observed age overestimations (Lang and Zolitschka, 2001; Shulmeister et al., 2001; Juschus et al., 2007).

Thomsen et al. (2008) have identified IRSL signals which show a lower laboratory fading rate compared to that normally used (typically stimulated at ~50 °C, IR_{50} and measured in the blue wavelength part of the spectrum, e.g. van Heteren et al., 2000; Auclair et al., 2007; Buylaert et al., 2007, 2011a). Thomsen et al. (2008) proposed the use of a post-IR IRSL signal stimulated at elevated temperature. Buylaert et al. (2009) tested this suggestion using a first stimulation at 50 °C (IR_{50}) and a second stimulation at 225 °C ($pIRIR_{225}$; preheat 250 °C for 60 s) and found that the observed (smaller) $pIRIR_{225}$ fading rates correlated with larger apparent burial doses. As a result of the investigations by Murray et al. (2009), Thiel et al. (2011) used a higher temperature preheat (320 °C for 60 s) and thus were able to increase their second stimulation temperature to 290 °C ($pIRIR_{290}$). Using these parameters they examined the natural signal from a loess sample of non-finite luminescence age (i.e. a sample in which the absorbed dose should give a natural signal in saturation on the laboratory dose response curve). Their Fig. 5 shows that this natural signal is indeed consistent with the saturation light level; this is only possible if the $pIRIR_{290}$ signal did not fade significantly over the burial lifetime of the sample. Thomsen et al. (2011) confirmed this observation for K-rich feldspar extracted from non-finite marine sand, and Buylaert et al. (2012) tested the accuracy of 36 ages based on this method against independent age control. They demonstrated that it was inappropriate to make any fading correction to $pIRIR_{290}$ data.

In this study we employ the same SAR $pIRIR_{290}$ protocol used by Buylaert et al. (2012) to measure the natural dose (D_e) (summarised in Table 1, protocol A). We also make use of a conventional SAR IR_{50} protocol (protocol B) (e.g. Buylaert et al., 2008, 2012).

4.2. Sample preparation and analytical facilities

Fig. 1 locates the 47 luminescence samples on the 5022-1D core log. Ohlendorf et al. (2011) have described the way in

Table 1
SAR protocols used to measure D_e values of K-feldspar extracts.

Step	A $pIRIR_{290}$	B IR_{50}
1	Dose	Dose
2	Preheat (320 °C for 60 s)	Preheat (250 °C for 60 s)
3	IRSL, 200 s at 50 °C	IRSL, 200 s at 50 °C → L_x
4	IRSL, 200 s at 290 °C → L_x	–
5[a]	Test dose	Test dose
6	Preheat (320 °C for 60 s)	Preheat (250 °C for 60 s)
7	IRSL, 200 s at 50 °C	IRSL, 200 s at 50 °C → T_x
8	IRSL, 200 s at 290 °C → T_x	–
9	IRSL, 200 s at 325 °C	IRSL, 200 s at 290 °C
10	Return to step 1	Return to step 1

[a] The test dose size ranged between 26 and 40 Gy.

which the core was split and sampled for luminescence dating in the Bremen laboratory (Germany). Care was taken to sample only the inner non-light exposed part of the sediment core and to avoid any influence of smearing by the core barrel. Each sample taken for luminescence represents ~20 cm of core length and no samples were taken close to boundaries of obvious lithological changes. A separate sample for dose rate analysis was taken over the entire range of the luminescence sample.

In the laboratory the samples were wet sieved to extract grains in the size range 63–250 μm. These fractions were treated with HCl and H_2O_2 to remove carbonates and organic material, respectively. A K-rich feldspar fraction was floated off using an aqueous heavy liquid (sodium heteropolytungstate 'LST Fastfloat'; density 2.58 g/cm^3). This fraction was cleaned with 10% HF for 40 min to remove coatings and the outer alpha irradiated layer. The heavy fraction was treated with concentrated (40%) HF for 1 h. This gave a clean quartz fraction (see Section 5.2). Grains were mounted in a single layer in a 8 mm diameter circle using silicone oil on either stainless steel cups (8.3 mm inner diameter) or discs (9.8 mm diameter). This gave aliquots each containing many hundreds to thousands of grains.

Luminescence measurements employed Risø TL/OSL readers model DA-20 (Bøtter-Jensen et al., 2010) equipped with blue LEDs (470 nm, ~80 mW/cm^2) infrared (IR) LEDs (870 nm, ~135 mW/cm^2) and each equipped with an accurately calibrated ^{90}Y/^{90}Sr beta source. Quartz OSL was detected through 7.5 mm of Schott U-340 (UV) glass filter and feldspar (post-IR) IRSL through a combination of Corning 7–59 and Schott BG-39 glass filters (blue–violet part of the spectrum). IR_{50} and $pIRIR_{290}$ signals are derived from the integral of the first 2 s of 200 s of IR stimulation, less a background based on the last 50 s.

The dose rate samples (~200 g dry weight, ~80 g in some cases where material was limited) were homogenised by grinding and mixed with hot wax before casting in a fixed geometry. The resulting solid cup- or disc-shaped samples were stored for >3 weeks to allow build-up of ^{222}Rn before counting for at least 24 h on a high resolution gamma spectrometer (Murray et al., 1987) to give measurements of the concentrations of U and Th series and ^{40}K.

5. Results

5.1. Dosimetry

The observed radionuclide concentrations are summarised in Table 2 and Fig. 2a–c. There is remarkably little variation with depth in the concentrations of ^{226}Ra (daughter of ^{238}U) and ^{232}Th; ^{40}K is a little more variable at about 15 m, possibly influenced by core disturbance and for sample 105719 the presence of redeposited Réclus tephra which is rich in K (Fig. 1). By normalising to ^{232}Th (Fig. 2d, e) we can reduce the dependence of concentration variation with grain size (because ^{232}Th tends to be bound to surfaces, and thus is related to surface area). The ^{226}Ra/^{232}Th ratio is significantly less variable with depth, although there is a clear systematic trend close to the surface, which we attribute to a probable loss of ^{226}Ra to the overlying water column. Zolitschka et al. (2006) showed that the lake is slightly salty at present (salinity ~3 mS cm^{-1}). It is known that ^{226}Ra is mobile in the presence of dissolved salts (e.g. Hancock and Murray, 1996) and thus could be mobilised by pore-water mixing with the overlying water column. There is no corresponding decrease in the ^{40}K/^{232}Th ratio compared to the ^{40}K concentrations alone, consistent with the idea that potassium is mainly found as part of the mineral structure (e.g. in feldspar), rather than on the grain surfaces.

These radionuclide concentrations have been converted into beta and gamma dose rates using the data given in Olley et al. (1996) and modified by the life-time burial water content using the expressions given in Aitken (1985) prior to be summed to give the total dose rates. Fig. 2f summarises the observed water contents (expressed as weight %). There is a clear smooth trend of decreasing water content with depth, and we take this to reflect the compaction of the sediment with increased burial depth. Thus we presume that the sediment was deposited with a water content of ~60% (modern near lake-floor value) and this decreased with time, so that by the time the sediment has acquired 100 m of overburden, the water content has dropped to ~20%. To derive the life-time average water content we simply calculate a running average down the core, in which each subsequent layer is averaged with the overlying average water content. This gives the data represented by the filled circles in Fig. 2f, and these data are used in subsequent calculations. The significance of this assumption is discussed further in Section 6. Because of the water depth of the lake (~100 m) the contribution of the cosmic dose rate (Prescott and Hutton, 1994) is negligible, at least for most of the burial time under consideration here. Finally an internal beta dose rate is calculated based on an assumed internal potassium content of 12.5 ± 0.5% in our K-feldspar extracts (based on the assumptions of Huntley and Baril, 1997) and the grain-size dependence of Mejdahl (1979); a Rb content of 400 ± 100 ppm was also assumed (Huntley and Hancock, 2001). K-feldspar grains are not entirely free from U and Th (e.g. Zhao and Li, 2005); an assumed effective internal alpha dose rate contribution from U and Th of 0.06 ± 0.03 Gy/ka was also included. The resulting total dose rates do not vary significantly with depth, and are summarised in Fig. 2g and Table 2.

5.2. Quartz OSL

Previous luminescence work on one of the Laguna Potrok Aike cores suggested that no quartz could be extracted from the sediment (Haberzettl et al., 2009). However, we successfully extracted pure sand-sized (90–180 μm) quartz grains from our samples (OSL IR depletion ratio of 1.04 ± 0.03, n = 3; Duller, 2003). A representative blue-light stimulated natural decay curve for the lowest sample in the core (105,701, ~96 m hole depth) is shown in Fig. 3. Unfortunately, the signal is not dominated by a fast component (the inset shows a normalised comparison with the fast-component dominated Risø calibration quartz). Reliable dose measurements using quartz are thus not possible and no further investigations using the quartz separates were made.

5.3. Feldspar (post-IR) IRSL

5.3.1. Luminescence properties of the IR_{50} and $pIRIR_{290}$ signals

Although we have no sample of non-finite luminescence age from this core, the related catchment study (Kliem et al., 2013a) reports the $pIRIR_{290}$ dating of a sample taken from a sand wedge. The natural luminescence signal is interpolated onto the dose response curve for an aliquot of this sample in Fig. 4a (taken from Kliem et al., 2013a). The $pIRIR_{290}$ natural signal is indistinguishable from saturation (mean ratio natural to saturation intensity = 0.98 ± 0.02; n = 5) confirming the stability of the $pIRIR_{290}$ signal in the sediments of this catchment. The inset shows the natural signal and dose response of the IR_{50} signal for this material.

The inset to Fig. 4b shows typical natural and regenerated $pIRIR_{290}$ luminescence decay curves for the deepest core sample (105701, Fig. 1) and the resulting sensitivity-corrected $pIRIR_{290}$ dose response curve is presented in Fig. 4b. The sensitivity-corrected

Table 2
Summary of depth information, sample codes, radionuclide concentrations, observed and modelled water contents, IR_{50} and $pIRIR_{290}$ D_e values and luminescence ages. Grain size of K-feldspar extract was 90–180 μm for all samples except for samples 115711, −13, −36 (63–180 μm) and sample 105737 (63–250 μm). Total dose rates include the beta dose rate from internal ^{40}K assuming an effective K content of 12.5 ± 0.5% (Huntley and Baril, 1997). The absolute uncertainty on the water content is ±4%. For more details on the dose-rate calculation see Section 5.1 in the main text. The $pIRIR_{290}$ D_e values have a residual dose of 12.6 ± 0.7 Gy subtracted from the measured value. The IR_{50} D_e values and the $pIRIR_{290}$ ages are not corrected for fading (see Section 5.3.2 in the main text).

Core hole depth (m)	Sample code			^{226}Ra (Bq/kg)	^{232}Th (Bq/kg)	^{40}K (Bq/kg)	Obs. w.c. (%)	Mod. w.c. (%)	Total dose rate (Gy/ka)	D_e, IR_{50} (Gy)	(*n*)	D_e, $pIRIR_{290}$ (Gy)	(*n*)	Age, $pIRIR_{290}$ (ka)	
0.53	10	57	32	15.7 ± 1.3	29.9 ± 1.4	468 ± 19	63	63	1.90 ± 0.07	13 ± 2[a]	10	45 ± 6	9	24 ± 3	R
0.84	10	57	33	15.4 ± 0.6	25.0 ± 0.7	455 ± 13	62	63	1.83 ± 0.06	5.7 ± 0.6	11	23 ± 2	8	12.6 ± 1.3	R
1.23	10	57	34	17.1 ± 1.1	23.2 ± 1.2	411 ± 16	61	62	1.77 ± 0.06	5.0 ± 0.2	12	12 ± 2	11	6.5 ± 1.0	R
1.73	10	57	30	14.6 ± 0.8	20.5 ± 0.8	395 ± 15	59	61	1.65 ± 0.06	5.9 ± 0.4	9	13 ± 2	15	7.9 ± 1.1	R
2.67	10	57	31	21.1 ± 0.8	28.1 ± 0.9	464 ± 14	56	60	1.95 ± 0.06	11.7 ± 0.8	14	32 ± 3	14	16.4 ± 1.4	R
3.22	10	57	28	21.3 ± 0.7	28.8 ± 0.8	467 ± 12	55	59	2.01 ± 0.06	11.7 ± 0.8	14	40 ± 3	14	20 ± 2	R
4.13	10	57	29	16.3 ± 1.1	18.6 ± 1.2	341 ± 14	52	58	1.64 ± 0.06	7.5 ± 0.2	15	18 ± 2	15	11.0 ± 1.2	R
4.64	10	57	26	16.8 ± 0.8	21.4 ± 0.8	388 ± 15	51	57	1.78 ± 0.06	10.5 ± 1.0[a]	9	33 ± 4	9	19 ± 3	R
5.29	10	57	27	17.7 ± 0.6	21.0 ± 0.6	351 ± 11	50	57	1.64 ± 0.06	13.5 ± 0.4	9	31 ± 2	12	19 ± 2	R
6.17	10	57	24	16.7 ± 0.5	18.8 ± 0.5	375 ± 10	48	56	1.67 ± 0.05	11.0 ± 0.3	13	14.5 ± 1.1	12	8.7 ± 0.7	
6.87	10	57	25	19.8 ± 0.6	24.4 ± 0.7	413 ± 11	47	55	1.82 ± 0.06	11.6 ± 0.9	9	19 ± 3	12	10.7 ± 1.5	R
8.14	10	57	23	22.0 ± 0.8	25.6 ± 0.9	414 ± 13	45	54	1.92 ± 0.06	11.5 ± 0.4	9	33 ± 4	18	17 ± 2	R,T
13.85	10	57	19	17.2 ± 0.6	20.9 ± 0.7	579 ± 14	36	53	2.10 ± 0.07	20 ± 2[a]	11	38 ± 4	12	18 ± 2	R
14.62	10	57	20	21.5 ± 0.5	29.7 ± 0.7	420 ± 10	37	52	1.98 ± 0.06	18.1 ± 0.5	9	34 ± 5	12	17 ± 2	R
18.40	10	57	18	18.5 ± 0.6	26.4 ± 0.7	213 ± 11	35	50	1.89 ± 0.06	29.4 ± 0.9	13	36 ± 2	12	19.3 ± 1.1	
18.97	12	57	15	19.1 ± 0.5	25.3 ± 0.6	424 ± 10	–	50	1.94 ± 0.06	32.5 ± 0.8	6	34 ± 2	12	17.5 ± 1.0	
21.26	10	57	17	20.9 ± 0.5	25.3 ± 0.6	415 ± 10	33	49	1.94 ± 0.06	33.7 ± 1.1	9	39 ± 2	11	20.4 ± 1.1	
23.12	10	57	16	19.5 ± 0.5	26.3 ± 0.6	396 ± 9	32	48	1.91 ± 0.06	33.2 ± 1.1	9	43.3 ± 1.2	12	22.6 ± 1.0	
24.33	10	57	15	20.1 ± 0.6	25.5 ± 0.7	414 ± 11	31	47	1.95 ± 0.06	35.3 ± 1.2	9	42 ± 2	11	21.7 ± 1.2	
26.05	12	57	02	18.0 ± 0.6	24.3 ± 0.6	372 ± 12	–	47	1.84 ± 0.06	37 ± 3	6	49.3 ± 1.0	12	26.8 ± 1.0	
27.26	10	57	14	18.7 ± 0.4	24.6 ± 0.4	394 ± 7	30	46	1.87 ± 0.06	39.2 ± 1.0	9	46 ± 2	12	24.4 ± 1.2	
30.30	10	57	13	19.0 ± 0.4	24.9 ± 0.5	394 ± 9	29	46	1.90 ± 0.06	47.4 ± 1.2	13	54.3 ± 1.4	11	28.7 ± 1.2	
34.14	10	57	12	18.8 ± 0.6	24.7 ± 0.7	389 ± 10	28	45	1.89 ± 0.06	37.9 ± 1.2[a]	12	57.8 ± 1.3	12	30.6 ± 1.2	R
36.71	10	57	11	19.2 ± 0.5	24.1 ± 0.6	370 ± 9	27	45	1.86 ± 0.06	47.8 ± 1.8	9	65 ± 2	11	35.2 ± 1.5	
37.12	12	57	16	18.1 ± 0.4	23.4 ± 0.5	363 ± 8	–	45	1.80 ± 0.06	55.4 ± 1.1	6	69 ± 2	12	38 ± 2	
41.24	12	57	10	18.6 ± 0.6	24.0 ± 0.7	395 ± 10	–	44	1.90 ± 0.06	58 ± 2	3	75 ± 2	9	39 ± 2	
41.75	10	57	10	19.8 ± 0.5	25.2 ± 0.6	388 ± 10	26	44	1.93 ± 0.06	54.6 ± 1.4	13	69 ± 2	11	35.6 ± 1.4	
42.19	10	57	09	19.6 ± 0.5	25.1 ± 0.6	378 ± 10	26	43	1.92 ± 0.06	54.0 ± 1.6	9	73 ± 2	12	38 ± 2	
44.08	12	57	04	20.4 ± 0.5	26.7 ± 0.6	381 ± 9	–	42	1.96 ± 0.06	62.1 ± 1.3	3	107 ± 8	9	55 ± 5	R
46.23	10	57	08	18.2 ± 0.5	24.5 ± 0.6	383 ± 9	25	42	1.89 ± 0.06	64.0 ± 1.5	9	87 ± 3	14	46 ± 2	
47.56	12	57	05	17.5 ± 0.6	21.8 ± 0.7	334 ± 10	–	42	1.78 ± 0.06	67.5 ± 0.9	6	90 ± 3	12	51 ± 2	
53.53	12	57	06	17.2 ± 0.5	22.4 ± 0.6	344 ± 9	–	43	1.77 ± 0.06	66 ± 2	3	92 ± 5	9	52 ± 3	
54.93	10	57	07	17.7 ± 0.4	23.1 ± 0.5	352 ± 8	24	42	1.82 ± 0.06	68 ± 2	9	90 ± 4	14	49 ± 3	
56.76	10	57	06	15.0 ± 0.5	21.6 ± 0.6	403 ± 10	24	41	1.87 ± 0.06	76.5 ± 1.1	7	136 ± 10	14	73 ± 6	R,T
59.03	12	57	07	18.9 ± 0.5	25.2 ± 0.5	357 ± 10	–	40	1.91 ± 0.06	83 ± 3	6	116 ± 4	12	61 ± 3	
61.50	12	57	08	20.2 ± 0.7	23.0 ± 0.7	313 ± 10	–	40	1.76 ± 0.06	63 ± 2	3	91 ± 3	9	52 ± 2	
62.20	10	57	05	20.4 ± 0.5	24.7 ± 0.6	362 ± 9	23	40	1.92 ± 0.06	66.1 ± 1.1	9	98 ± 4	15	51 ± 3	
63.46	10	57	35	21.3 ± 0.5	27.7 ± 0.6	394 ± 9	23	40	2.02 ± 0.07	74 ± 2	10	139 ± 4	11	69 ± 3	R
64.35	12	57	13	19.4 ± 0.5	23.6 ± 0.5	357 ± 10	–	39	1.87 ± 0.06	95 ± 4	6	137 ± 6	11	74 ± 4	T
65.74	10	57	04	20.6 ± 0.4	25.1 ± 0.5	359 ± 7	23	39	1.91 ± 0.06	78 ± 3	8	117 ± 4	14	61 ± 3	
72.33	10	57	03	21.5 ± 0.5	28.1 ± 0.6	371 ± 9	22	38	1.99 ± 0.07	70 ± 9	3	113 ± 2	15	56 ± 2	
73.36	12	57	09	21.5 ± 0.5	26.3 ± 0.6	406 ± 10	–	38	2.05 ± 0.07	82 ± 2	6	130 ± 3	12	63 ± 3	
83.27	10	57	37	14.7 ± 0.4	17.2 ± 0.4	309 ± 7	21	38	1.65 ± 0.06	71.0 ± 1.1	8	105 ± 4	11	64 ± 3	
87.51	10	57	02	19.0 ± 0.4	24.4 ± 0.5	366 ± 8	21	37	1.92 ± 0.06	89 ± 3	9	130 ± 4	15	68 ± 3	
91.76	12	57	14	20.6 ± 0.7	24.9 ± 0.8	337 ± 11	–	37	1.89 ± 0.07	93 ± 3	6	135 ± 4	12	71 ± 3	
92.36	10	57	36	20.1 ± 0.5	24.8 ± 0.5	364 ± 9	21	37	1.97 ± 0.07	80.2 ± 1.7[a]	12	134 ± 3	12	68 ± 3	R
96.48	10	57	01	22.1 ± 0.7	27.2 ± 0.8	362 ± 12	20	36	1.98 ± 0.07	86.6 ± 1.2	9	128 ± 3	15	64 ± 3	

Notes: (*n*) denotes the number of aliquots contributing to the D_e.
Uncertainties represent 1 standard error; radionuclide concentrations and D_e values are quoted with only random uncertainties, total dose rates and ages include systematic components.
R = rejected sample based on $IR_{50}/pIRIR_{290}$ ratio (Fig. 7b); T = turbidite.
[a] Due to a lack of material the IR_{50} measurements could not be carried out using a low preheat (protocol B, Table 1). Instead the IR_{50} D_e values derived as part of the $pIRIR_{290}$ protocol (protocol A, Table 1) were used. Buylaert et al. (2012) have shown on 35 samples that the IR_{50} D_e values measured as part of the $pIRIR_{290}$ protocol yield D_e values that are within 7% of the IR_{50} D_e's measured with a single IR_{50} SAR (protocol B) despite poor dose recovery. For the purpose of the bleaching argument (see Section 5.3.3 and Fig. 7b) we consider these values sufficiently accurate.

natural signal lies at ~30% of signal saturation; i.e. well inside the dating range for this mineral. The average SAR $pIRIR_{290}$ recycling ratio (61 aliquots from 16 samples) is 1.005 ± 0.003 (see Fig. 5a) and recuperation is <3% of the sensitivity corrected natural signal (inset Fig. 5a). We have undertaken dose recovery tests (Wallinga et al., 2000; Murray and Wintle, 2003) to test the ability of our SAR protocols to measure a known dose given in the laboratory. A beta dose of 45 Gy was given to aliquots of the youngest samples (105724 and 105730). This dose was then measured in the usual manner (protocols A and B in Table 1). After subtraction of the appropriate natural dose, the ratio of the measured dose to the given dose is 1.05 ± 0.05 (n = 12) for the $pIRIR_{290}$ protocol and 1.02 ± 0.02 (n = 3, only sample 105730 was used) for the IR_{50} protocol; these results indicate that our protocols can accurately measure a known dose given before any thermal treatment.

We next test for the presence of an unbleachable residual signal in our data. Sohbati et al. (2012) and Buylaert et al. (2012) have shown that there may be a difficult-to-bleach component in a post-IR IRSL signal (both $pIRIR_{225}$ and $pIRIR_{290}$). If such a signal exists it is likely to be a characteristic of the material and should not depend on the subsequent burial dose. Any such unbleachable residual must be subtracted from all our results before consideration of

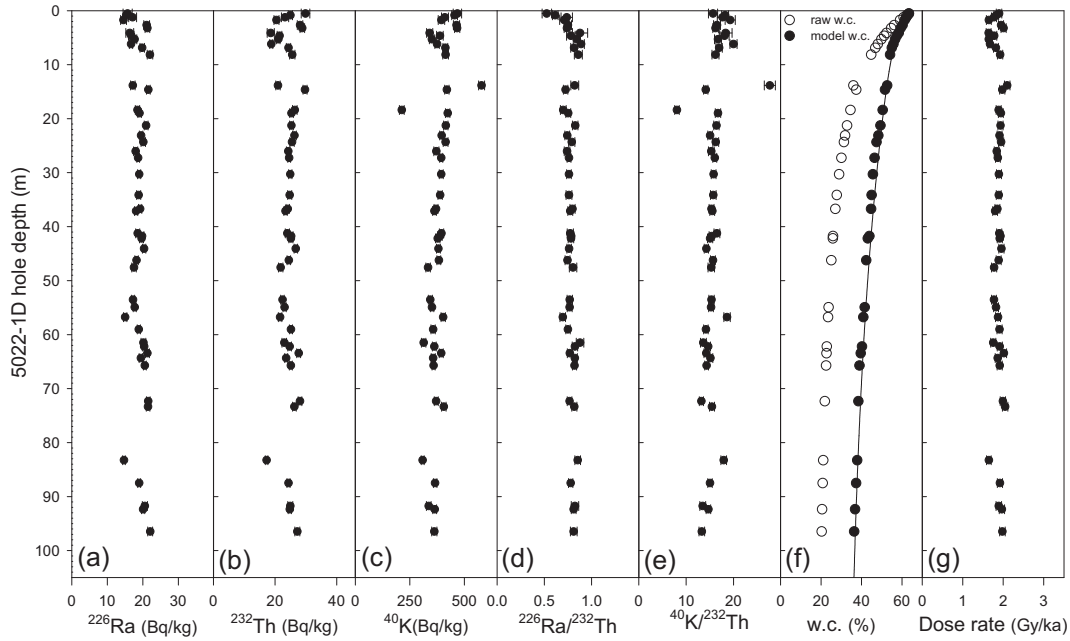

Fig. 2. Summary of dosimetric information. 'w.c.' is water content expressed as a percentage of dry weight. 'Dose rate' is the total field dose rate to sand-sized K-feldspar grains. Analytical data are provided with Table 2.

fading or incomplete bleaching. To test this we have exposed aliquots of 24 different samples taken over the entire core each for 4 h to an artificial daylight spectrum (Hönle SOL2 solar simulator) approximately 6 times more intense than full sunlight. The apparent residual doses after bleaching were then measured in the usual manner and the average residual dose for each sample is plotted against the measured natural dose in Fig. 5b. There is no significant trend in these data and the mean residual $pIRIR_{290}$ dose is 12.6 ± 0.7 Gy ($n = 24$). This value has been subtracted from the mean measured values of D_e to give the presumed dose acquired since last light exposure (Table 2). It seems likely to us that this residual dose arises from thermal transfer, a mechanism first proposed for this signal by Buylaert et al. (2011b) as a result of studies on modern/young fine-grained samples from China.

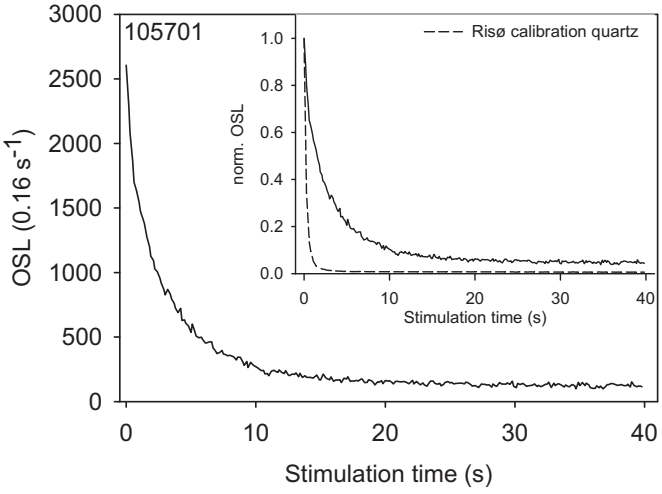

Fig. 3. Natural blue-light stimulated luminescence decay curve of a large aliquot of sand-sized quartz extracted from sample 105701. The purity of the quartz extract was confirmed by the OSL IR depletion ratio of Duller (2003). The inset shows the same data together with a decay curve of calibration quartz, both curves normalised to their initial intensity.

Qin and Zhou (2012) have suggested that this thermal transfer process has the potential to impact on the accuracy of post-IR IRSL dating, although they acknowledge that any potential interference will be reduced by increasing the test dose size relative to the natural dose. Buylaert et al. (2012) have investigated the effect of test dose size on a range of 35 mainly sand-sized known-age samples (their Fig. 3c and d); they do not observe any correlation between the ratio of measured to expected dose and either test-dose size or cumulative sensitivity change and their measured doses are consistent with expected doses. This absence of effect may have arisen because Buylaert et al. (2012) used a 325 °C IR clean-out step at the end of each SAR cycle, as is used in this study (but in contrast to Qin and Zhou, 2012). In addition our test doses are at least 30% of the natural $pIRIR_{290}$ dose. Thus it seems unlikely that the interference identified by Qin and Zhou (2012) plays a significant role in our results but, as always, the only reliable way to test the importance of such a mechanism is by comparison with independent age control.

5.3.2. *Stability of the IR_{50} and $pIRIR_{290}$ signals*

Although there is good evidence that the $pIRIR_{290}$ signal is stable over the age range of interest here (see Fig. 4a), we have made measurements of $pIRIR_{290}$ signal stability over laboratory timescales (fading rate or g value measurements, Aitken, 1985). The fading rate using SAR (protocol A in Table 1) (Auclair et al., 2003) was determined on the same aliquots used for D_e measurement; the regeneration dose for fading measurements was 100 Gy and the test dose 40 Gy. The g values were normalised to a measurement time of 2 days after irradiation (Huntley and Lamothe, 2001). Fig. 5c presents a histogram summarising all g_{2days} values obtained on 15 samples (at least 3 aliquots per sample) selected over the entire core depth. The inset shows an example of a g value measurement on an aliquot of sample 105701. The mean g_{2days} value is small (0.62 ± 0.06%/decade, $n = 45$) but finite. A 0.6%/decade fading rate would imply a ~6% correction to the ages using the model of Huntley and Lamothe (2001). Buylaert et al. (2012) also report finite g_{2days} values (1.44 ± 0.03%/decade, $n = 128$) but nevertheless argued that the $pIRIR_{290}$ ages should not be corrected for fading.

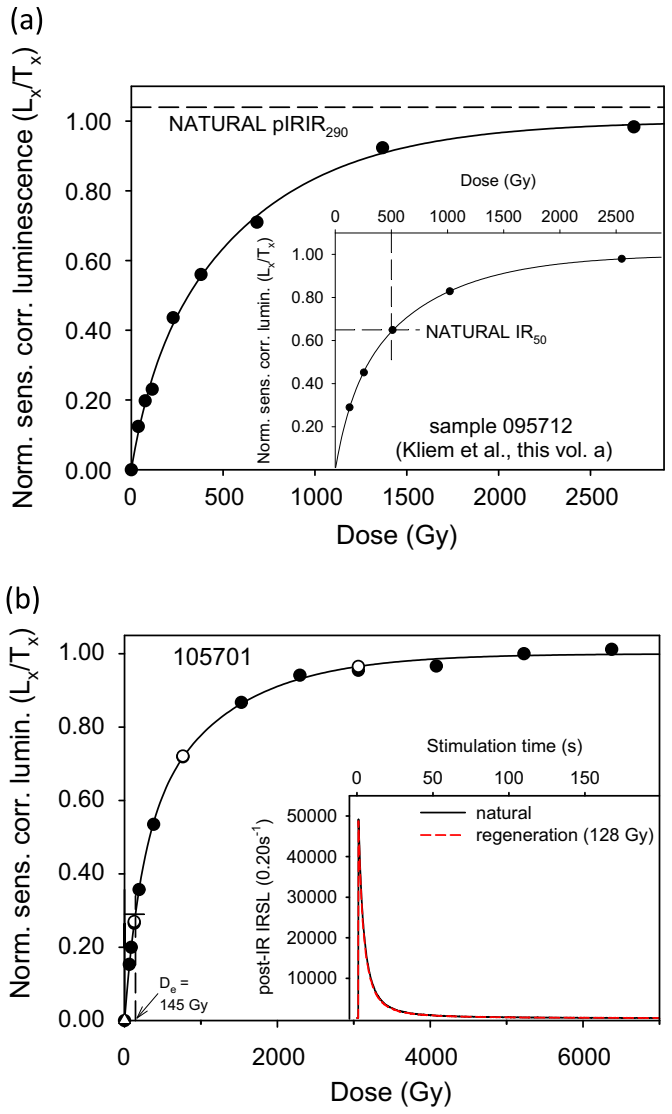

Fig. 4. (a) Normalised sensitivity corrected $pIRIR_{290}$ dose response curve for an aliquot of sample 095712 (from Kliem et al., 2013a). The inset shows the IR_{50} dose response curve (measured with protocol B, Table 1) for another aliquot of this sample. Dashed lines show the natural normalised sensitivity corrected signal levels. Both dose response curves were fitted with the sum of two exponential functions of the form $y = a(1 - \exp(-bx)) + c(1 - \exp(-dx))$. The sensitivity corrected luminescence (L_x/T_x) values were normalised to the fitted saturation value ($a + c$). (b) Normalised sensitivity corrected $pIRIR_{290}$ dose response curve for an aliquot of sample 105701 (hole depth, ~96 m). Interpolation of the sensitivity corrected natural luminescence level on the dose response curve (dashed line) gives the D_e value for this aliquot. Open circles represent remeasured dose points (to give the recycling ratio) and the open triangle is the response to a zero dose (recuperation). The inset shows natural and regenerated $pIRIR_{290}$ decay curves for this sample.

This argument was based on the observations of (i) similar apparent fading rates for fast component dominated quartz OSL signals, (ii) natural $pIRIR_{290}$ signals in saturation for samples of non-finite luminescence age (see also Fig. 4a) and (iii) good agreement between uncorrected $pIRIR_{290}$ ages and age control for 36 samples. They suggest that it is possible that these apparent laboratory fading rates are in fact a measurement artefact, perhaps associated with uncorrected sensitivity change. In this study we follow Buylaert et al. (2012) and do not correct the $pIRIR_{290}$ ages (Table 2).

In contrast to the $pIRIR_{290}$ signal, the IR_{50} signal is known to be unstable as a result of athermal fading (discussed above). The

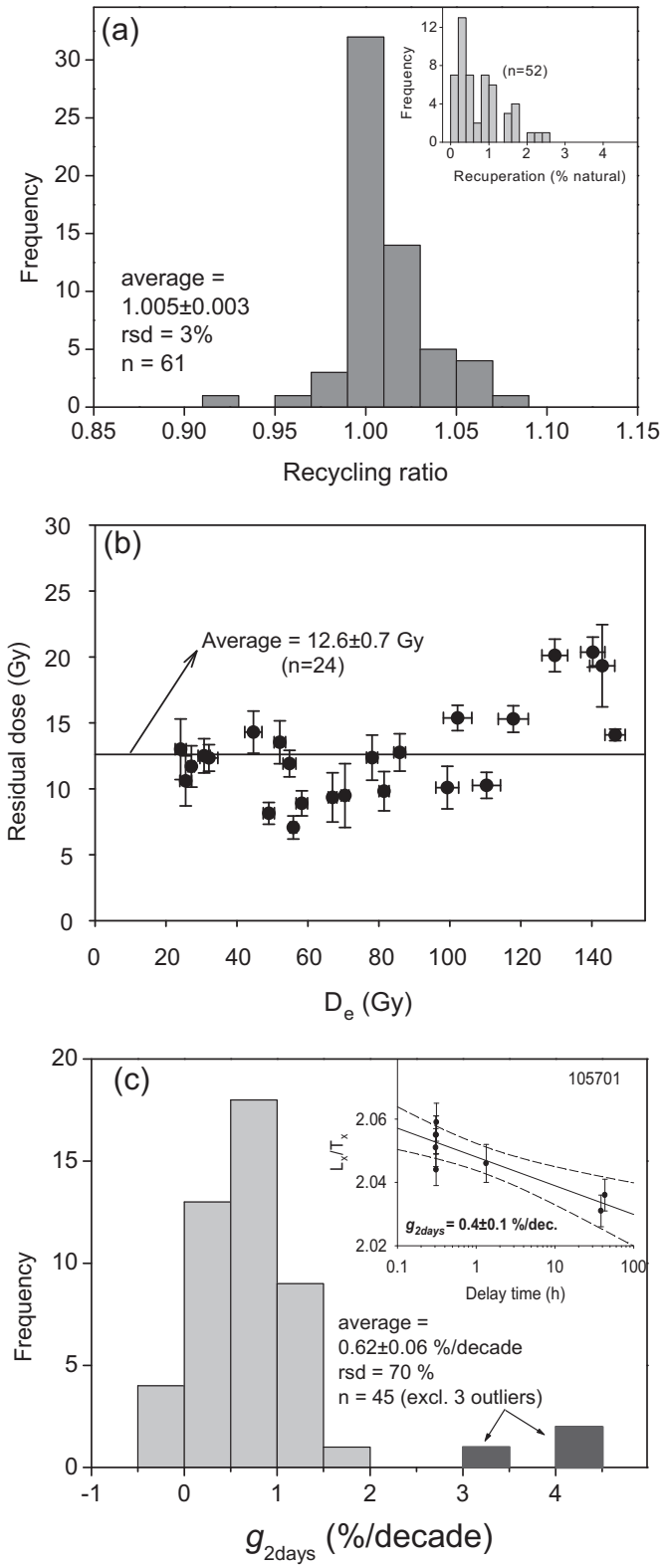

Fig. 5. (a) Histogram summarising the recycling ratios. The inset shows a histogram of the recuperation values. (b) Residual $pIRIR_{290}$ dose measured after 4 h SOL2 bleaching plotted as a function of the natural $pIRIR_{290}$ dose for a selection of samples taken over the entire core length. Error bars represent standard errors. The mean value is plotted as a horizontal straight line. (c) Histogram summarising the fading rates (g_{2days} values) with an example of a fading rate measurement on a single aliquot shown inset.

average IR_{50} fading rate (measured using protocol B; Table 1) for 25 samples is 4.16 ± 0.11%/decade (n = 72). Because of the large correction factors implied, any ages calculated using these equivalent doses are considered much less reliable and are not presented. Our position is supported by the luminescence ages presented in Haberzettl et al. (2009) which make use of an IR_{50} signal to calculate ages. Some of these ages are consistent with other dating methods and some are gross underestimates (see Figs. 3 and 5 in Haberzettl et al., 2009); this is what would be expected from a combination of poor bleaching and inaccurate correction for athermal fading. However, our IR_{50} equivalent doses (Table 2) are used in the next section in the discussion of incomplete bleaching.

5.3.3. Post-IR IR_{290} ages and detecting poor bleaching

The $pIRIR_{290}$ ages are presented against core depth in Fig. 6 as open and closed circles. Between about 15 and 55 m the ages increase smoothly with depth but in the younger section (apparently post-LGM) and at about 60 m there is considerable scatter in the ages. It seems likely that most of the scatter results from age overestimation, perhaps because of poor bleaching.

One way to examine whether or not the $pIRIR_{290}$ signal is likely to have been fully bleached or reset is to compare with other luminescence signals that have different sensitivities to daylight. It is known that the IR_{50} signal bleaches more rapidly in sunlight than IR signals stimulated at elevated temperature (Thomsen et al., 2008) or the $pIRIR_{290}$ signal (Buylaert et al., 2012; Murray et al., 2012). We have measured the relative bleaching of the two signals here by exposing natural aliquots of sample 105701 to artificial daylight for various lengths of time; the normalised sensitivity-corrected signals remaining after these exposures are shown in Fig. 7a. As expected, the IR_{50} signal from this material bleaches very much faster than the $pIRIR_{290}$ signal; after ~1000 s of light exposure the normalised IR_{50} signal has been reduced to about a tenth of the corresponding $pIRIR_{290}$ signal. Thiel et al. (2011) suggested that the different IR_{50} to $pIRIR_{290}$ D_e ratio for one of their samples compared to the other samples in their study may be due to

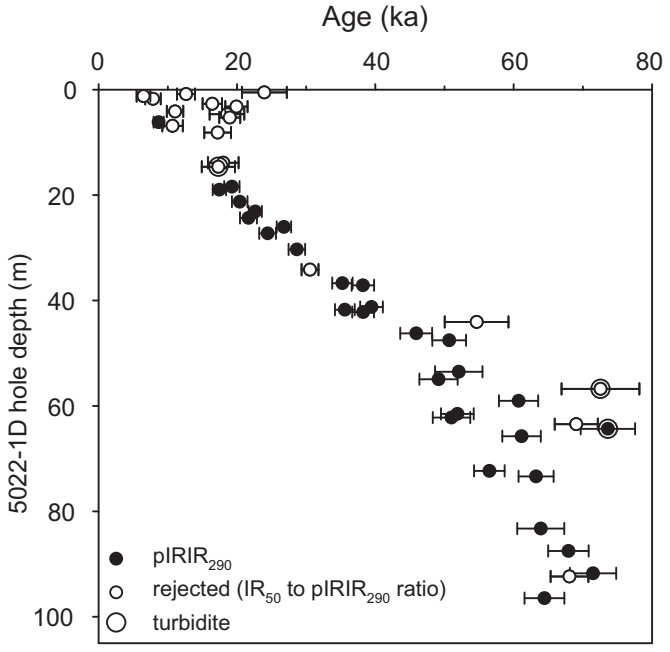

Fig. 6. Post-IR IR_{290} ages plotted against core depth for the PASADO 5022-1D core. Open circles represent those samples which are rejected based on their IR_{50} to $pIRIR_{290}$ dose ratio (see Fig. 7b and Section 5.3.3).

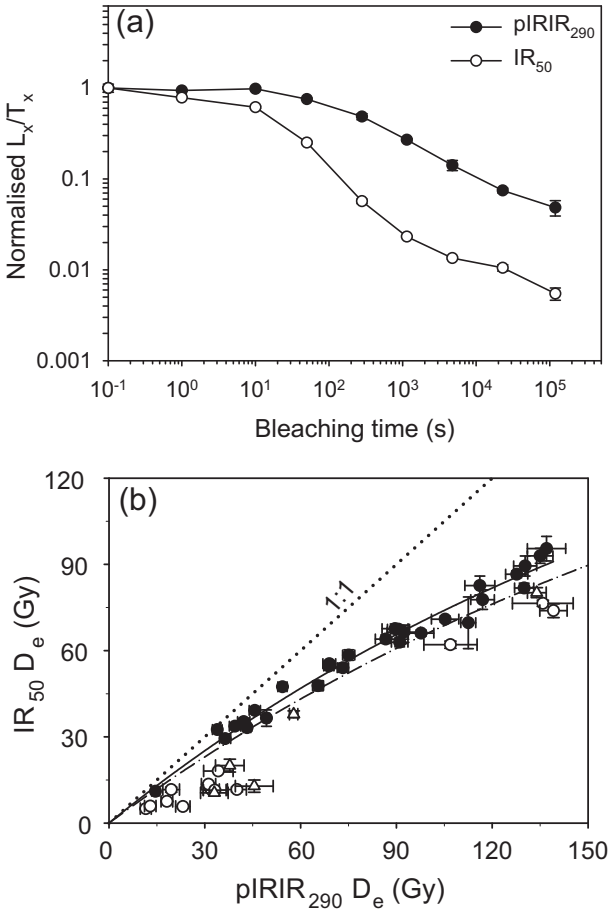

Fig. 7. (a) Post-IR IR_{290} and IR_{50} bleaching curves measured for sample 105701 using protocols A and B in Table 1, respectively. Aliquots were exposed for different lengths of time to a Hönle SOL2 solar simulator and their sensitivity-corrected luminescence was measured. The data are normalised to the natural sensitivity-corrected luminescence (zero exposure time). Each data-point is the average of three aliquots and error bars represent one standard error. (b) Sample-averaged uncorrected IR_{50} and $pIRIR_{290}$ D_e values plotted against each other. The solid line represents a single saturating exponential function of the form $y = a(1 - \exp(-bx))$ fitted to the data represented by the solid symbols; the dash-dotted line is derived from the solid line by multiplying the $pIRIR_{290}$ co-ordinates of the line by 1.1. Open symbols represent those samples rejected because they lie more than 10% away from the solid line (along x-axis) and are not within one standard deviation of the line. Regression was first undertaken using all data; samples were then rejected as above and the regression repeated using only the accepted data. This process was repeated until no further samples were rejected (three iterations were needed and only the end-result is shown here). Triangles represent those 5 samples for which the IR_{50} D_e values were derived from the $pIRIR_{290}$ measurement sequence (see notes to Table 2 for details). Error bars represent one standard error (see Table 2).

incomplete bleaching of the $pIRIR_{290}$ signal during post-depositional reworking. Fig. 7b shows the IR_{50} equivalent doses plotted against the $pIRIR_{290}$ doses for all the Potrok Aike lake samples; the majority of these data (filled symbols) lie on a smooth curve (solid line) below the line of unit slope (dotted line), consistent with the effects of anomalous fading. However, some data points (open symbols) plot significantly below this smooth correlation, consistent with these $pIRIR_{290}$ signals being less well-bleached than the corresponding IR_{50} signals. We have chosen to reject all data that lie more than one standard deviation below a line running 10% below the solid line (dash-dotted line in Fig. 7b; the solid line was fitted using an iterative process, see caption to Fig. 7b). While this rejection criterion is arbitrary, it is applied non-subjectively to all our data; we do not use absolute dose values or stratigraphic information to identify the rejected samples (shown

as open symbols in Figs. 7b and 6). We regard the rejected samples as likely to be incompletely bleached and these are not considered further.

6. Discussion

The results of Section 5.3.1 show that our SAR pIRIR$_{290}$ protocol is suitable for the measurement of the dose using K-rich feldspar extracts from this lacustrine sediment core. We also deduce that the pIRIR$_{290}$ signal from a sample taken from within the catchment area is stable (Fig. 4a); it is likely that this result applies to the lake sediments as well. However, the results of Fig. 6 (open and filled symbols) indicate that the pIRIR$_{290}$ was not always fully reset before deposition. In the previous section we identified 29 samples (out of 47) for which the IR$_{50}$ and the pIRIR$_{290}$ signals were almost certainly bleached to some constant value before deposition (filled circles in Figs. 6 and 7b). Sediment transport and sedimentation processes vary considerably in space and time. Bleaching resulting from these processes must be heterogeneous; individual sediment grains will either show different degrees of bleaching or be completely bleached. It is very difficult to imagine an incomplete-bleaching process that would result in such uniform bleaching of these two signals over many tens of thousands of years; it seems very much more probable that we can regard these 29 samples as well-bleached.

It is important to realise that we identify outliers non-subjectively (that is, without looking at the age information). In our model the ratio of IR$_{50}$ to pIRIR$_{290}$ doses from well-bleached samples should lie on a smooth curve. Incompletely bleached samples should lie below this curve because the pIRIR$_{290}$ doses should be too large compared to those from the more easily-bleached IR$_{50}$ signal – if we reject points that plot furthest away (along the *x*-axis) from the solid line in Fig. 7b we are rejecting the least well-bleached samples. By progressively rejecting samples that lie closer and closer to the solid line we progressively reject better and better bleached samples. Eventually of course, because of random scatter, we will start to reject samples that are well-bleached. Rejecting well-bleached samples is a waste of data but should not systematically bias our final age–depth curve.

It is interesting to note that of the three samples taken from unambiguously identified turbidite layers in this core (105706, 105720 and 125713), two have been rejected on the grounds of incomplete bleaching; this suggests that these turbidite layers originate from an unusual transport event during which the transported sediment received only a limited amount of light exposure. This is in contrast to the third turbidite sample (125713) which appears to contain well-bleached material; presumably this layer resulted from sub-aquatic reworking of previously deposited well-bleached material. Nevertheless, sample 125713 was rejected from the age model because its genetic origin may mean it is not in its correct stratigraphic position.

The ages accepted as most likely to be reliable vary smoothly with depth (Fig. 8) to about 65 ka at the bottom of the core. These ages are of course dependent on the water content model (see Section 5.1) in which we assumed that compaction (dewatering) occurred as a result of increased overburden. This is a likely explanation but to investigate the importance of this assumption we can consider the two limiting cases of (i) the raw water contents measured in the core were present at deposition and applied throughout the lifetime of the site (i.e. no natural dewatering) or (ii) dewatering occurred primarily as a result of coring and that the field water contents before sampling were closer to the lake floor value of ~60%. Using these two limiting assumptions gives an average underestimate of age, using (i) above, of 7% compared to the results of Table 2 with a maximum deviation of 10% at the bottom of the core. Using (ii) above gives an average overestimate of age of 6% with a maximum deviation of 13% again at the bottom of the core. It is unlikely that some natural dewatering did not occur and so it is correspondingly unlikely that the true ages deviate from our preferred values (Table 2) by such large fractions. These upper limits to our systematic uncertainties arising from these two very unlikely water content histories should also be compared with an average total uncertainty on individual ages of about 8%. We conclude that the total uncertainties given in Table 2 are likely to cover any realistic systematic error arising from water content history.

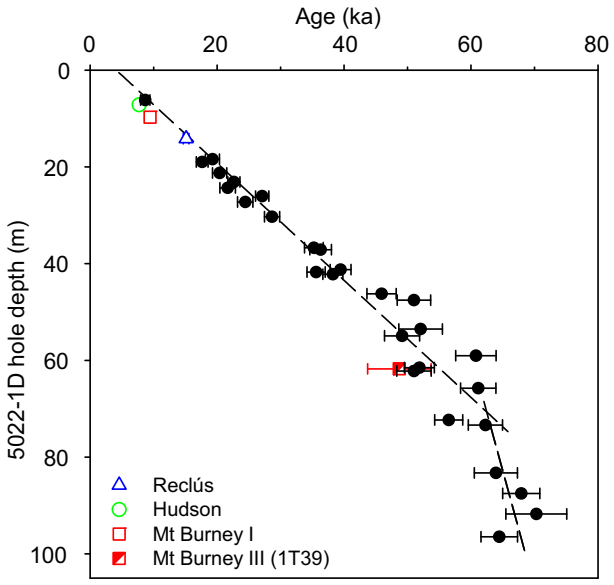

Fig. 8. Accepted pIRIR$_{290}$ ages plotted against core depth (depth below lake floor) for the PASADO 5022-1D core together with the available tephrochronological age control (Stern, 2008; Haberzettl et al., 2009; Kliem et al., 2013b). Linear regression through the luminescence ages of the samples above and below 80 m hole depth are shown as dashed lines.

Fig. 8 also shows that the average sedimentation rate over the past almost 60 ka has been remarkably constant. All of the sample ages lying above 80 m hole depth are consistent with the straight line (upper dashed line) regressed through the data of slope 1.21 ± 0.02 m ka^{-1}. Before about 60 ka the apparent sedimentation rate was significantly higher (~5 m ka^{-1}, lower dashed line), and ~65 ka ago at least 20 m of sediment was deposited over a period of time that is small compared to our age uncertainties (of ~5 ka in this interval). We also note that our chosen criterion for identifying incompletely bleached samples may be too strict; at least three samples (105712, 105725 and 105736) are rejected although the pIRIR$_{290}$ ages are consistent with the linear correlation shown in Fig. 8 (compare with open circles at ~7 m, ~34 m, ~92 m in Fig. 6; Table 2).

To test the conclusion that the selected pIRIR$_{290}$ ages are reliable it is also important to verify our accepted ages against the independent age control provided by tephra ages (also shown in Fig. 8). It is clear that our pIRIR$_{290}$ ages are completely consistent with all four independently dated tephras identified in core 5022-1D. This agreement with independent age control suggests that the selected samples are indeed well-bleached and give accurate estimates of age.

Nevertheless, regression of the data above 80 m also suggests that the top of the core was deposited 4.1 ± 0.9 ka ago. Although some of this intercept must arise because the sediment/water interface was not recovered in this core, even a missing 1 m would only account for an intercept of 1.2 ka. We do not consider it likely

that this intercept reflects a significant degree of unidentified incomplete bleaching. This would require that all samples down to ~80 m were incompletely bleached by some process that resulted in uniform (incomplete) bleaching of these two signals over some 60 ka; this was rejected above as unlikely. There are two much more credible explanations for the remaining intercept: (i) our laboratory-based measurement of the unbleachable residual is an underestimate of the field condition or (ii) the very recent sedimentation rate does not follow the pattern of the last 60 ka – the latter is in our view the more likely explanation.

7. Conclusion

The SAR $pIRIR_{290}$ protocol used in this paper passed all laboratory tests (recycling, recuperation, dose recovery) and gave a natural $pIRIR_{290}$ signal from a sample of known non-finite luminescence age in saturation (Fig. 4a); this is a strong indication of signal stability over the time range of interest in this study. The new objective criterion for identification and rejection of poorly bleached samples yielded a stratigraphically consistent luminescence age–depth data set which is in good agreement with independent age control. The age–depth curve varies smoothly with depth, and indicates a remarkably constant ~1.2 m ka^{-1} accumulation rate over the last ~60 ka, with a much larger rate for some time before that. We suggest that these data should provide a reliable basis for an age model for the Laguna Potrok Aike PASADO core 5022-1D. After firmly linking this core with the PASADO composite profile 5022-2CP, the luminescence ages will be applied to confirm or improve the radiocarbon-based age–depth model (Kliem et al., 2013b).

Acknowledgements

Pierre Kliem is thanked for help with subsampling of the core and for providing the water content values. We thank Vicki Hansen, Anne-Birgit Sørensen and Mette Adrian for sample preparation and help with the luminescence and gamma spectrometry measurements. This research is supported by the International Continental Scientific Drilling Program (ICDP) in the framework of the "Potrok Aike Maar Lake Sediment Archive Drilling Project" (PASADO). Funding for drilling was provided by the ICDP, the German Science Foundation (DFG), the Swiss National Funds (SNF), the Natural Sciences and Engineering Research Council of Canada (NSERC), the Swedish Vetenskapsradet (VR) and the University of Bremen. Jan-Pieter Buylaert thanks The Danish Independent Research Council for support (Steno grant no. 11-104566). Four anonymous reviewers and guest-editor Pierre Francus are thanked for their comments that helped to improve the paper.

References

Aitken, M.J., 1985. Thermoluminescence Dating. Academic Press, London.
Aitken, M.J., 1998. An Introduction to Optical Dating. Oxford University Press, Oxford.
Anselmetti, F.S., Ariztegui, D., De Batist, M., Gebhardt, A.C., Haberzettl, T., Niessen, F., Ohlendorf, C., Zolitschka, B., 2009. Environmental history of southern Patagonia unravelled by the seismic stratigraphy of Laguna Potrok Aike. Sedimentology 56, 873–892.
Auclair, M., Lamothe, M., Huot, S., 2003. Measurement of anomalous fading for feldspar IRSL using SAR. Radiation Measurements 37, 487–492.
Auclair, M., Lamothe, M., Lagroix, F., Banerjee, S.K., 2007. Luminescence investigations of loess and tephra from Halfway House section, Central Alaska. Quaternary Geochronology 2, 34–38.
Buylaert, J.P., Vandenberghe, D., Murray, A.S., Huot, S., De Corte, F., Van den haute, P., 2007. Luminescence dating of old (>70 ka) Chinese loess: a comparison of single-aliquot OSL and IRSL techniques. Quaternary Geochronology 2, 9–14.
Buylaert, J.P., Murray, A.S., Huot, S., 2008. Optical dating of an Eemian site in northern Russia using K-feldspar. Radiation Measurements 43, 715–720.
Buylaert, J.P., Murray, A.S., Thomsen, K.J., Jain, M., 2009. Testing the potential of an elevated temperature IRSL signal from K-feldspar. Radiation Measurements 44, 560–565.
Buylaert, J.P., Huot, S., Murray, A.S., Van den haute, P., 2011a. Infrared stimulated luminescence dating of an Eemian (MIS 5e) site in Denmark using K-feldspar. Boreas 40, 46–56.
Buylaert, J.P., Thiel, C., Murray, A.S., Vandenberghe, D.A.G., Yi, S., Lu, H., 2011b. IRSL and post-IR IRSL residual doses recorded in modern dust samples from the Chinese Loess Plateau. Geochronometria 38, 432–440.
Buylaert, J.P., Jain, M., Murray, A.S., Thomsen, K.J., Thiel, C., Sohbati, R., 2012. A robust feldspar luminescence dating method for Middle and Late Pleistocene sediments. Boreas 41, 435–451.
Bøtter-Jensen, L., Thomsen, K.J., Jain, M., 2010. Review of optically stimulated luminescence (OSL) instrumental developments for retrospective dosimetry. Radiation Measurements 45, 253–257.
Davids, F., Duller, G.A.T., Roberts, H.M., 2010. Testing the use of feldspars for optical dating of hurricane overwash deposits. Quaternary Geochronology 5, 125–130.
Duller, G.A.T., 2003. Distinguishing quartz and feldspar in single grain luminescence measurements. Radiation Measurements 37, 161–165.
Duller, G.A.T., 2004. Luminescence dating of Quaternary sediments: recent advances. Journal of Quaternary Science 19, 183–192.
Forman, S.L., Pierson, J., Gómez, J., Brigham-Grette, J., Nowaczyk, N.R., Melles, M., 2007. Luminescence geochronology for sediments from Lake El'gygytgyn, northeast Siberia, Russia: constraining the timing of paleoenvironmental events for the past 200 ka. Journal of Paleolimnology 37, 77–88.
Gebhardt, A.C., Ohlendorf, C., Niessen, F., De Batist, M., Anselmetti, F.S., Ariztegui, D., Kliem, P., Wastegård, S., Zolitschka, B., 2012. Seismic evidence of up to 200 m lake-level change in southern Patagonia since Marine Isotope Stage 4. Sedimentology 59, 1087–1100.
Godfrey-Smith, D.L., Huntley, D.J., Chen, W.H., 1988. Optically dating studies of quartz and feldspar sediment extracts. Quaternary Science Reviews 7, 373–380.
Haberzettl, T., Corbella, H., Fey, M., Janssen, S., Lücke, A., Mayr, C., Ohlendorf, C., Schäbitz, F., Schleser, G., Wille, M., Wulf, S., Zolitschka, B., 2007. Wet-dry cycles in southern Patagonia -chronology, sedimentology and geochemistry of a lacustrine sediment record from Laguna Potrok Aike (Argentina). Holocene 17, 297–311.
Haberzettl, T., Anselmetti, F.S., Bowen, S.W., Fey, M., Mayr, C., Zolitschka, B., Arizegui, D., Mauz, B., Ohlendorf, C., Kastner, S., Lücke, A., Schäbitz, F., Wille, M., 2009. Late Pleistocene dust deposition in the Patagonian steppe – extending and refining the paleoenvironmental and tephrochronological record from Laguna Potrok Aike back to 55 ka. Quaternary Science Reviews 28, 2927–2939.
Hahn, A., Kliem, P., Ohlendorf, C., Zolitschka, B., Rosen, P., The PASADO Science Team, 2013. Climate induced changes as registered in inorganic and organic sediment components from Laguna Potrok Aike (Argentina) during the past 51 ka. Quaternary Science Reviews 71, 154–166. http://dx.doi.org/10.1016/j.quascirev.2012.09.015.
Hancock, G.J., Murray, A.S., 1996. Source and distribution of dissolved radium in the Bega River estuary, southeastern Australia. Earth and Planetary Science Letters 138, 145–155.
Huntley, D.J., Baril, M.R., 1997. The K content of the K-feldspars being measured in optical dating or in thermoluminescence dating. Ancient TL 15, 11–13.
Huntley, D.J., Hancock, R.G.V., 2001. The Rb contents of the K-feldspar grains being measured in optical dating. Ancient TL 19, 43–46.
Huntley, D.J., Lamothe, M., 2001. Ubiquity of anomalous fading in K-feldspars and the measurement and correction for it in optical dating. Canadian Journal of Earth Sciences 38, 1093–1106.
Huntley, D.J., Lian, O.B., 2006. Some observations on tunnelling of trapped electrons in feldspars and their implications for optical dating. Quaternary Science Reviews 25, 2503–2512.
Jain, M., Ankjærgaard, C., 2011. Towards a non-fading signal in feldspar: insight into charge transport and tunnelling from time-resolved optically stimulated luminescence. Radiation Measurements 46, 292–309.
Jain, M., Murray, A.S., Bøtter-Jensen, L., 2003. Characterisation of blue-light stimulated luminescence components in different quartz samples: implications for dose measurement. Radiation Measurements 37, 441–449.
Juschus, O., Preusser, F., Melles, M., Radtke, U., 2007. Applying SAR-IRSL methodology for dating fine-grained sediments from Lake El'gygytgyn, north-eastern Siberia. Quaternary Geochronology 2, 187–194.
Kliem, P., Buylaert, J.-P., Hahn, A., Mayr, C., Murray, A.S., Ohlendorf, C., Veres, D., Wastegård, S., Zolitschka, B., The PASADO Science Team, 2013a. Magnitude, geomorphologic response and climate links of lake level oscillations at Laguna Potrok Aike, Patagonian steppe (Argentina). Quaternary Science Reviews 71, 131–146. http://dx.doi.org/10.1016/j.quascirev.2012.08.023.
Kliem, P., Enters, D., Hahn, A., Ohlendorf, C., Lisé-Pronovost, A., St-Onge, G., Wastegård, S., Zolitschka, B., The PASADO Science Team, 2013b. Lithology, radiocarbon chronology and sedimentological interpretation of the lacustrine record from Laguna Potrok Aike, southern Patagonia. Quaternary Science Reviews 71, 54–69. http://dx.doi.org/10.1016/j.quascirev.2012.07.019.
Lamothe, M., 2004. Optical dating of pottery, burnt stones, and sediments from selected Quebec archaeological sites. Canadian Journal of Earth Sciences 41, 659–667.
Lang, A., Zolitschka, B., 2001. Optical dating of annually laminated lake sediments: a test case from Holzmaar/Germany. Quaternary Science Reviews 20, 737–742.
Li, B., Li, S.-H., 2011. Luminescence dating of K-feldspar from sediments: a protocol without anomalous fading correction. Quaternary Geochronology 6, 468–479.

Li, B., Li, S.H., Wintle, A.G., Zhao, H., 2008. Isochron dating of sediments using luminescence of K-feldspar grains. Journal of Geophysical Research 113, F02026.
Madsen, A.T., Murray, A.S., 2009. Optically stimulated luminescence dating of young sediments: a review. Geomorphology 109, 3–16.
Madsen, A.T., Buylaert, J.P., Murray, A.S., 2011. Luminescence dating of young coastal deposits from New Zealand using feldspar. Geochronometria 38, 378–390.
Mayr, C., Wille, M., Haberzettl, T., Fey, M., Janssen, S., Lücke, A., Ohlendorf, C., Oliva, G., Schäbitz, F., Schleser, G.H., Zolitschka, B., 2007. Holocene variability of the Southern Hemisphere westerlies in Argentinean Patagonia (52°S). Quaternary Science Reviews 26, 579–584.
Mejdahl, V., 1979. Thermoluminescence dating: beta-dose attenuation in quartz grains. Archaeometry 21, 61–72.
Morthekai, P., Jain, M., Murray, A.S., Thomsen, K.J., Bøtter-Jensen, L., 2008. Fading characteristics of martian analogue materials and the applicability of a correction procedure. Radiation Measurements 43, 672–678.
Moska, P., Poręba, G., Bluszcz, A., Wiszniowska, A., 2008. Combined IRSL/OSL dating on fine grains from Lake Baikal sediments. Geochronometria 31, 39–43.
Murray, A.S., Olley, J.M., 2002. Precision and accuracy in the optically stimulated luminescence dating of sedimentary quartz: a status review. Geochronometria 21, 1–16.
Murray, A.S., Wintle, A.G., 1999. Isothermal decay of optically stimulated luminescence in quartz. Radiation Measurements 30, 119–125.
Murray, A.S., Wintle, A.G., 2000. Luminescence dating of quartz using an improved single-aliquot regenerative-dose protocol. Radiation Measurements 32, 57–73.
Murray, A.S., Wintle, A.G., 2003. The single aliquot regeneration dose protocol: potential for improvements in reliability. Radiation Measurements 37, 377–381.
Murray, A.S., Marten, R., Johnston, A., Martin, P., 1987. Analysis for naturally occurring radionuclides at environmental concentrations by gamma spectrometry. Journal of Radioanalytical and Nuclear Chemistry 115, 263–288.
Murray, A.S., Buylaert, J.P., Thomsen, K.J., Jain, M., 2009. The effect of preheating on the IRSL signal from feldspar. Radiation Measurements 44, 554–559.
Murray, A.S., Thomsen, K.J., Masuda, N., Buylaert, J.P., Jain, M., 2012. Identifying well-bleached quartz using the different bleaching rates of quartz and feldspar luminescence signals. Radiation Measurements 47, 688–695.
Ohlendorf, C., Gebhardt, C., Hahn, A., Kliem, P., Zolitschka, B., The PASADO Science Team, 2011. The PASADO core processing strategy — a proposed new protocol for sediment core treatment in multidisciplinary lake drilling projects. Sedimentary Geology 239, 104–115.
Ohlendorf, O., Fey, M., Gebhardt, C., Haberzettl, T., Lücke, A., Mayr, C., Schäbitz, F., Wille, M., Zolitschka, B., 2013. Mechanisms of lake-level change at Laguna Potrok Aike (Argentina) – insights from hydrological balance calculations. Quaternary Science Reviews 71, 27–45. http://dx.doi.org/10.1016/j.quascirev.2012.10.040.
Olley, J.M., Murray, A.S., Roberts, R.G., 1996. The effects of disequilibria in the uranium and thorium decay chains on the burial dose rates in fluvial sediments. Quaternary Science Reviews 15, 751–760.
Prescott, J.R., Hutton, J.T., 1994. Cosmic ray contributions to dose rates for luminescence and ESR dating: large depths and long-term variations. Radiation Measurements 23, 497–500.
Preusser, F., Chithambo, M.L., Gotte, T., Martini, M., Ramseyer, K., Sendezera, E.J., Susino, G.J., Wintle, A.G., 2009. Quartz as a natural luminescence dosimeter. Earth-Science Reviews 97, 184–214.
Qin, J.T., Zhou, L.P., 2012. Effects of thermally transferred signals in the post-IR IRSL SAR protocol. Radiation Measurements 47, 710–715.
Recasens, C., Ariztegui, D., Gebhardt, A.C., Gogorza, C., Haberzettl, T., Hahn, A., Kliem, P., Lisé-Pronovost, A., Lücke, A., Maidana, N., Mayr, C., Ohlendorf, C., Schäbitz, F., St-Onge, G., Wille, M., Zolitschka, B., The PASADO Science Team, 2012. New insights into paleoenvironmental changes in Laguna Potrok Aike, Southern Patagonia, since the Late Pleistocene: the PASADO multiproxy record. The Holocene 22, 1322–1335. http://dx.doi.org/10.1177/0959683611429833.
Reimann, T., Tsukamoto, S., Naumann, M., Frechen, M., 2011. The potential of using K-rich feldspars for optical dating of young coastal sediments – a test case from Darss-Zingst peninsula (southern Baltic Sea coast). Quaternary Geochronology 6, 207–222.
Shulmeister, J., Shane, P., Lian, O., Okuda, M., Carter, J.A., Harper, M., Dickinson, W., Augustinus, P., Heijnis, H., 2001. A long late-Quaternary record from Lake Poukawa, Hawke's Bay, New Zealand. Palaeogeography, Palaeoclimatlology, Palaeoecology 176, 81–107.
Singarayer, J.S., Bailey, R.M., 2003. Further investigations of the quartz optically stimulated luminescence components using linear modulation. Radiation Measurements 37, 451–458.
Sohbati, R., Murray, A.S., Buylaert, J.-P., Ortuno, M., Cunha, P.P., Masana, E., 2012. Luminescence dating of Pleistocene alluvial sediments affected by the Alhama de Murcia fault (eastern Betics, Spain) – a comparison between OSL, IRSL and post-IR IRSL ages. Boreas 41, 250–262.
Spooner, N.A., 1994. The anomalous fading of infrared-stimulated luminescence from feldspars. Radiation Measurements 23, 625–632.
Stern, C.R., 2008. Holocene tephrochronology record of large explosive eruptions in the southernmost Patagonian Andes. Bulletin of Volcanology 70, 435–454.
Thiel, C., Buylaert, J.-P., Murray, A., Terhorst, B., Hofer, I., Tsukamoto, S., Frechen, M., 2011. Luminescence dating of the stratzing loess profile (Austria) – testing the potential of an elevated temperature post-IR IRSL protocol. Quaternary International 234, 23–31.
Thomas, P.J., Murray, A.S., Sandgren, P., 2003. Age limit and age underestimation using different OSL signals from lacustrine quartz and polymineral fine grains. Quaternary Science Reviews 22, 1139–1143.
Thomsen, K.J., Murray, A.S., Jain, M., Bøtter-Jensen, L., 2008. Laboratory fading rates of various luminescence signals from feldspar-rich sediment extracts. Radiation Measurements 43, 1474–1486.
Thomsen, K.J., Murray, A.S., Jain, M., 2011. Stability of IRSL signals from sedimentary K-feldspar samples. Geochronometria 38, 1–13.
van Heteren, S., Huntley, D.J., van de Plassche, O., Lubberts, R.K., 2000. Optical dating of dune sand for the study of sea-level change. Geology 28, 411–414.
Vandenberghe, D., Kasse, C., Hossain, M., De Corte, F., Van Den Haute, P., Fuchs, M., Murray, A.S., 2004. Exploring the method of optical dating and comparison of optical and ^{14}C ages of Late Weichselian coversands in the southern Netherlands. Journal of Quaternary Science 19, 73–86.
Wallinga, J., Murray, A., Duller, G., 2000. Underestimation of equivalent dose in single-aliquot optical dating of feldspars caused by preheating. Radiation Measurements 32, 691–695.
Wallinga, J., Bos, A.J.J., Dorenbos, P., Murray, A.S., Schokker, J., 2007. A test case for anomalous fading correction in IRSL dating. Quaternary Geochronology 2, 216–221.
Wintle, A.G., 1973. Anomalous fading of thermoluminescence in mineral samples. Nature 245, 143–144.
Wintle, A.G., 2008. Luminescence dating: where it has been and where it is going. Boreas 37, 471–482.
Wintle, A.G., Murray, A.S., 2006. A review of quartz optically stimulated luminescence characteristics and their relevance in single-aliquot regeneration dating protocols. Radiation Measurements 41, 369–391.
Zhao, H., Li, S.-H., 2005. Internal dose rate to K-feldspar grains from radioactive elements other than potassium. Radiation Measurements 40, 84–93.
Zolitschka, B., Schäbitz, F., Lücke, A., Corbella, H., Ercolano, B., Fey, M., Haberzettl, T., Janssen, S., Maidana, N., Mayr, C., Ohlendorf, C., Oliva, G., Paez, M.M., Schleser, G.H., Soto, J., Tiberi, P., Wille, M., 2006. Crater lakes of the Pali Aike Volcanic field as key sites for paleoclimatic and paleoecological reconstructions in southern Patagonia, Argentina. Journal of South American Earth Sciences 21, 294–309.
Zolitschka, B., Anselmetti, F., Ariztegui, D., Corbella, H., Francus, P., Ohlendorf, C., Schäbitz, F., PASADO Science Team, 2009. The Laguna Potrok Aike scientific drilling project PASADO (ICDP Expedition 5022). Scientific Drilling 8, 29–34.
Zolitschka, B., Anselmetti, F., Ariztegui, D., Corbella, H., Francus, P., Lücke, A., Maidana, N., Ohlendorf, C., Schäbitz, F., Wastegard, S., 2013. Environment and climate of the last 51,000 years – new insights from the Potrok Aike maar lake sediment archive drilling project (PASADO). Quaternary Science Reviews 71, 1–12. http://dx.doi.org/10.1016/j.quascirev.2012.11.024.